Applied Polymer SCIENCE

ARTICLE

Synthesis and Characterization of Poly(HEMA-*co*-MMA)-*g*-POSS Nanocomposites by Combination of Reversible Addition Fragmentation Chain Transfer Polymerization and Click Chemistry

Md. Rafiqul Islam,[1] Long Giang Bach,[1] Jong Myung Park,[2] Seong-Soo Hong,[3] Kwon Taek Lim[1]

[1]Department of Imaging System Engineering, Pukyong National University, Busan 608-737, Republic of Korea

[2]Surface Engineering Laboratory, Graduate Institute of Ferrous Technology, Pohang University of Science and Technology, Pohang 790-784, Republic of Korea

[3]Department of Chemical Engineering, Pukyong National University, Busan 608-739, Republic of Korea

Correspondence to: K. T. Lim (E-mail: ktlim@pknu.ac.kr)

ABSTRACT: New hybrid poly(hydroxyethyl methacrylate-*co*-methyl methacrylate)-*g*-polyhedral oligosilsesquioxane [poly(HEMA-*co*-MMA)-*g*-POSS] nanocomposites were synthesized by the combination of reversible addition fragmentation chain transfer (RAFT) polymerization and click chemistry using a *grafting to* protocol. Initially, the random copolymer poly(HEMA-*co*-MMA) was prepared by RAFT polymerization of HEMA and MMA. Alkynyl side groups were introduced onto the polymeric backbones by esterification reaction between 4-pentynoic acid and the hydroxyl groups on poly(HEMA-*co*-MMA). Azide-substituted POSS (POSS—N_3) was prepared by the reaction of chloropropyl-heptaisobutyl-substituted POSS with NaN_3. The click reaction of poly(HEMA-*co*-MMA)-alkyne and POSS—N_3 using CuBr/PMDEATA as a catalyst afforded poly(HEMA-*co*-MMA)-*g*-POSS. The structure of the organic/inorganic hybrid material was investigated by Fourier transformed infrared, ^{1}H-NMR, and ^{29}Si-NMR. The elemental mapping analysis of the hybrid using X-ray photoelectron spectroscopy and EDX also suggest the formation of poly(HEMA-*co*-MMA)-anchored POSS nanocomposites. The XRD spectrum of the nanocomposites gives evidence that the incorporation of POSS moiety leads to a hybrid physical structure. The morphological feature of the hybrid nanocomposites as captured by field emission scanning electron microscopy and transmission electron microscopic analyses indicate that a thick layer of polymer brushes was immobilized on the POSS cubic nanostructures. The gel permeation chromatography analysis of poly(HEMA-*co*-MMA) and poly(HEMA-*co*-MMA)-*g*-POSS further suggests the preparation of nanocomposites by the combination of RAFT and click chemistry. The thermogravimetric analysis revealed that the thermal property of the poly(HEMA-*co*-MMA) copolymer was significantly improved by the inclusion of POSS in the copolymer matrix. © 2012 Wiley Periodicals, Inc. J. Appl. Polym. Sci. 000: 000–000, 2012

KEYWORDS: hybrid nanocomposite; random copolymer; POSS; RAFT; click chemistry

Received 28 July 2011; accepted 13 February 2012; published online 00 Month 2012

DOI: 10.1002/app.37520

INTRODUCTION

The development of inorganic–organic hybrid nanocomposites has attracted great attention due to their prospect of improving the engineering properties of conventional materials and creating new properties. The synthesis of such materials with new properties and superior performance is a continually expanding research area, which covers subjects ranging from chemistry, physics, biology, to material science.[1–3] Hybrid materials based on polymers with nanoscale inorganic fillers are becoming more and more important in conventional engineering because of combining the functionality and processibility of an organic phase and enhanced thermal/chemical stability of an inorganic phase. Among various nanoparticles, hybrid inorganic–organic monomeric units, polyhedral oligosilsesquioxane (POSS) is a new class of advanced materials capable of forming various nanocomposites. The materials having POSS-moieties have found wide applications in dental and other medical materials, fire-retardant materials, space-resistant materials, photonics, low-dielectric materials, fuel cells, elastomers, electrolytes, laser materials, cosmetics, biology, and other applications.[4–9] Fully condensed POSS contains an inorganic Si—O core surrounded with various organic groups useful for tuning the surface chemistry and interaction with the host copolymer matrix. It is the combination of an inorganic core and the organic periphery

that provide unique physical and chemical properties to POSS compounds. Over the past decade, there has been a steadily increasing interest in the creation of POSS-based structures for use as blocks in molecular nanocomposite structures for a variety of applications. One advantage that POSS imparts is chemical versatility, allowing the compatibility between POSS nanoparticles and different polymeric matrixes.[10,11] Introducing POSS into a polymer backbone creates an interesting paradox in terms of desired properties. It was observed that the incorporation of POSS provided a polymer with excellent material properties, such as good oxidation resistance, superior surface hardness, extremely high thermal stability, reduced flammability, and enhanced mechanical strength leading to advanced organic/inorganic hybrid chemical feedstock.[12–15]

Poly(methyl methacrylate) (PMMA) and poly(2-hydroxyethyl-methacrylate) (PHEMA) are widely used polymers. PMMA has been used in diverse fields such as biomaterials, optoelectronics, and optic fibers because of its good optical (high transparency and clarity) and mechanical properties.[16] In contrast, PHEMA is most widely used hydrogel, since the water content is similar to living tissues. Moreover, its hydrophilicity basically from the hydroxyl functional group makes it bio- and blood-compatibility and develops resistance to degradation.[17] In addition, PHEMA has high oxygen permeability, good mechanical properties, and favorable refractive index value.[18] PMMA could be copolymerized with HEMA to tailor the hydrophilicity and wettability of PMMA, which can then be used in special applications, particularly, in solid-state pulsed dye lasers[19] and in biomedical fields.[20] The poly(MMA-*co*-HEMA) copolymers have been reported to synthesize by suspension and microemulsion systems.[21,22] However, recently, controlled/living radical polymerization (CRP) has got immense interest due to the well-defined architecture and narrow polydispersities of polymers. Among CRPs, RAFT is widely used because of its simplicity as well as vast functional group tolerance. In the recent years, grafting techniques have been used to attach polymers onto the surfaces of nano- and microparticles. POSS units can be incorporated into virtually all types of polymers either by blending, grafting, or copolymerization reactions.[23–29] In general, for chemical attachment, two different approaches can be categorized, the *grafting to* and the *grafting from* approach. In the *grafting from* technique, polymer chains grow from the initiators on the substrate, while polymer chains carry an active terminal group and are coupled to the active surface in the *grafting to* technique.

Recently, as a highly efficient organic reaction, the Cu(I)-catalyzed 1,3-dipolar cycloaddition reaction between azides and alkynes, known as "click reaction" have gained a great deal of attention due to their high specificity and nearly quantitative yields in the presence of many functional groups.[30–33] Click reactions have been widely used in macromolecular engineering and the synthesis of functional monomers and polymers, bioconjugated polymers, block and graft copolymers, dendrimers, cyclic polymers, star and brush copolymers, and networks.[34–37] The ease of the synthesis of alkyne and azide functionalities coupled with tolerance to a wide variety of functional groups and reaction conditions make this coupling process highly attractive for the modification of polymeric materials.

Combination of CRP and click chemistry offers an effective way to prepare functional polymeric materials. Several reports on the synthesis of (co)polymers via CRP and subsequent azide-alkyne-coupling reactions have been documented, but majority of these works were performed through the modification of (co)polymers prepared by ATRP.[38,39] On the other hand, only a few works have been accomplished using combination of RAFT and click chemistry so far.[40,41] However, those approaches are often accompanied with either troublesome deprotection or cumbersome postpolymerization modification.

In this article, we demonstrate the successful synthesis of a novel type of hybrid nanocomposite material poly(hydroxyethyl methacrylate-*co*-methyl methacrylate)-*g*-polyhedral oligosilsesquioxane [poly(MMA-*co*-HEMA)-*g*-POSS] by the *grafting to* method using the combination of RAFT and click reactions (Scheme 1).

EXPERIMENTAL

Materials

MMA (99%) and HEMA (97%) were purified by passing the liquid through a neutral alumina column to remove inhibitors before use. 2,2′-Azobisisobutyronitrile (AIBN; 97%) was recrystallized in methanol before use. 2-Cyano-2-propyl dodecyl trithiocarbonate (RAFT agent; 97%), chloropropyl–heptaisobutyl-substituted POSS (97%), *N*,*N*,*N*′,*N*″,*N*″-pentamethyl-diethylenetriamine (PMDETA; 99%), *N*,*N*′-dicyclohexylcarbodiimide (DCC; 99%), 4-dimethylaminopyridine (DMAP; 99%), and CuBr (98%) were used as received. All the above-mentioned chemicals were purchased from Aldrich, Yongin, Korea.

Azidation of Chloropropyl–Heptaisobutyl-Substituted POSS (POSS—N_3)

Chloropropyl–heptaisobutyl-substituted POSS (1.0 g, 1.12 mmol) and 15 mL of DMF were added into a round-bottomed flask. Sodium azide (0.360 g, 5.55 mmol) was added to the solution. After stirring for 24 h at 80°C, the reaction mixture was evaporated, diluted with tetrahydrofuran (THF), and precipitated in excess amount of methanol. The product was dried in a vacuum oven for 24 h at 35°C, giving 0.87 g of white solid.

Synthesis of Random Copolymer Poly(HEMA-*co*-MMA) via RAFT Technique

The synthesis of random copolymer poly(HEMA-*co*-MMA) was accomplished by using the ratio of reagents [MMA]/[HEMA]/[RAFT]/[AIBN] = 115/45/1/2. In a typical method, the RAFT agent (0.02 g, 0.06 mmol), AIBN (0.02 g, 0.12 mmol), HEMA (0.3 mL, 2.46 mmol), MMA (0.7 mL, 6.54 mmol) and dried THF (4 mL) were successively added into a 25-mL glass bottle with a magnetic bar. A predegassed reflux condenser with gas inlet/outlet was attached to the flask quickly, and the system was purged with argon through the solution for 30 min. The polymerization was allowed to proceed at 80°C while stirring under nitrogen atmosphere. After polymerization was carried out for 12 h, the reaction mixture was cooled to room temperature and precipitated in excess amount of hexane. The product was filtered and dried in a vacuum oven at room temperature overnight to get 0.84 g of solid product as determined by gravimetric measurement.

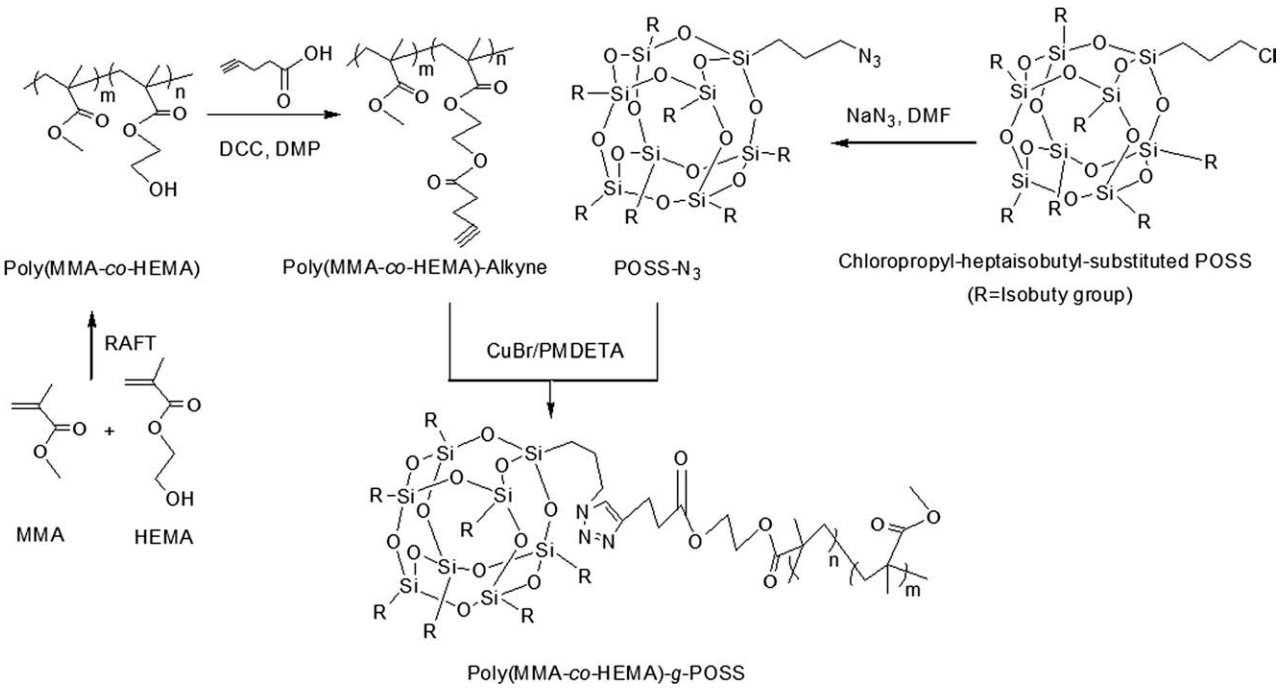

Scheme 1. Synthesis of poly(HEMA-*co*-MMA)-*g*-POSS via the combination of RAFT & Click Chemistry.

Synthesis of Alkyne-Functionalized Poly(HEMA-*co*-MMA)

Alkynyl side groups were introduced onto the polymeric backbones by esterification reaction between the hydroxyl groups on PHEMA and 4-pentynoic acid. In a typical procedure, random copolymer poly(HEMA-*co*-MMA) (1.0 g, 2.4 mmol for the HEMA unit), DCC (4.92 g, 24 mmol), and 4-pentynoic acid (1.17 g, 12 mmol) were added sequentially into 40 mL DMF before the flask was immersed into ice-water bath. Under magnetic stirring, 0.125 g DMAP solution in 3 mL DMF was added into the mixture within 5 min. The reaction mixture was allowed to stir for 36 h at room temperature. During this period, the reaction mixture slowly turned into brown, and the insoluble DCC urea precipitated out. After filtration to remove the solid, the polymer product was precipitated in excess amount of water to remove unreacted 4-pentynoic acid. After redissolving in THF, the polymers were precipitated again in excess amount of hexane to remove unreacted DCC and DCC urea. The product was dried in a vacuum oven for overnight at 35°C to obtain 0.927 g of the alkyne-functionalized copolymer.

Synthesis of Poly(HEMA-*co*-MMA)-*g*-POSS by Click Reaction Between POSS—N_3 and Poly(HEMA-*co*-MMA)-Alkyne

In a typical procedure for the synthesis of poly(HEMA-*co*-MMA)-*g*-POSS, POSS—N_3 (266 mg, 0.29 mmol), and poly (HEMA-*co*-MMA)-alkyne (53.2 mg, 0.08 mmol for the HEMA-alkyne unit) were taken in a 25-mL Schlenk flask containing 3 mL DMF, Cu Br (8 mg, 0.05 mmol), and PMDETA (10 mg, 0.05 mmol).[11] The reaction mixture was degassed by three freeze-pump-thaw cycles and stirred for 24 h at room temperature. After 24 h, the polymer solution was exposed to air, diluted with THF, and the crude product was passed through neutral alumina to remove copper complex. And then repeated precipitation in hexane and diethyl ether was carried out for the removal of unreacted POSS—N_3. The product was dried in a vacuum oven for overnight at 35°C to obtain 119 mg of white solid powder.

Characterization and Measurements

The changes in the surface chemical bonding of poly(HEMA-*co*-MMA), poly(HEMA-*co*-MMA)-Alkyne, POSS—Cl, POSS—N_3, and poly(HEMA-*co*-MMA)-*g*-POSS nanocomposites were analyzed by Fourier transformed infrared spectrophotometry (FTIR) using a BOMEM Hartman & Braun FTIR spectrometer in the frequency range of 4000–400 cm^{-1}. The elemental analysis of the hybrids was carried out by using a field emission scanning electron microscopy (FE–SEM) equipped with an energy-dispersive X-ray (EDX) spectrometer (HitachiJEOL-JSM-6700F system, Japan). All samples for SEM analysis were prepared by drying to fit in a specimen stub. The specimens were postfixed with an ultrathin coating of osmium by sputtering at 15 mA. The applied acc voltage was 15 kV. Transmission electron microscopy (TEM) images were recorded using a Joel JEM 2010 instrument (Japan) with an accelerating voltage of 80 kV. A drop of the solution in distilled ethanol was placed on a copper grid for the analysis. Thermogravimetric analysis (TGA) was conducted with a Perkin-Elmer Pyris 1 analyzer (USA). Before the test, all the samples were carefully grinded into fine powder. The sample size was 10–15 mg, and three experiments were conducted to collect one data point. The samples were scanned within the temperature range of 50–800°C at a heating rate of 10°C min^{-1} under continuous nitrogen flow. Surface composition was investigated using an X-ray photoelectron spectroscopy (XPS; Thermo VG Multilab 2000) in ultra high vacuum with Al Kα radiation. Gel permeation chromatography (GPC) was performed using an Agilent 1200 Series equipped with PLgel 5 μm MIXED-C columns, with THF as the solvent at 30°C. The solution flow rate was 1 mL/min. Calibration was carried out using

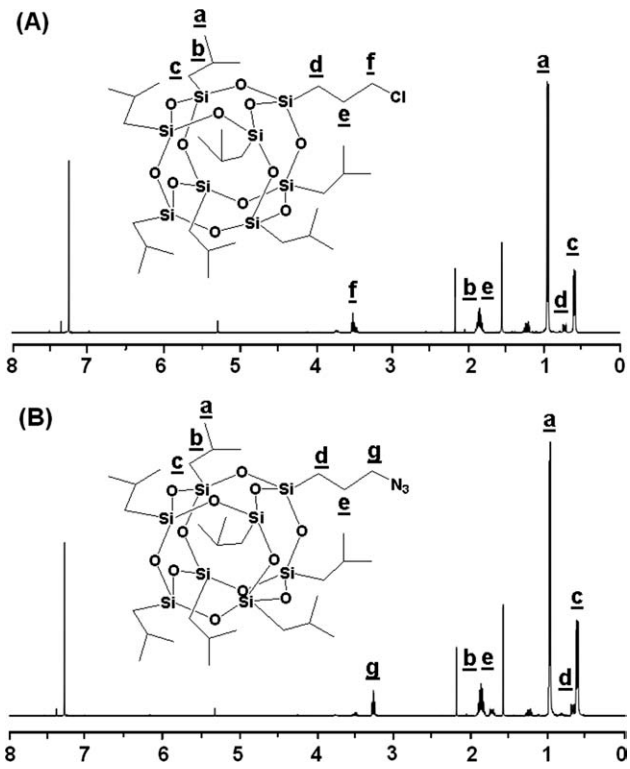

Figure 1. ^{1}H-NMR spectra of (A) POSS—Cl and (B) POSS—N_3.

PMMA standards. The ^{1}H-NMR spectra of poly(HEMA-*co*-MMA), poly(HEMA-*co*-MMA)-alkyne, POSS—Cl, POSS—N_3, and (MMA-*co*-HEMA)-*g*-POSS nanocomposites were recorded using a JNM-ECP 400 (JEOL) spectrophotometer with $CDCl_3$. The ^{29}Si-NMR spectra of POSS—N_3 and poly(HEMA-*co*-MMA)-*g*-POSS nanocomposites were obtained using a JEOL JNM–A400 (80 MHz) spectrometer.

RESULTS AND DISCUSSION

Synthesis and Characterization of POSS—N_3

A new type of hybrid nanocomposites of poly(MMA-*co*-HEMA) grafted with POSS was prepared using the Cu(I)-catalyzed via azide–alkyne click reaction strategy. We first carried out azidation of chloropropyl–heptaisobutyl-substituted POSS by the reaction of POSS—Cl with NaN_3 in DMF for 24 h at 80°C. Second, POSS—N_3 and poly(HEMA-*co*-MMA)-alkyne were clicked to give poly(HEMA-*co*-MMA)-*g*-POSS using CuBr/PMDETA as a catalyst at room temperature via the click reaction.

The terminal chloride atoms of POSS—Cl were easily transformed into azide groups to produce POSS—N_3 via the nucleophilic substitution reaction in DMF at room temperature. The typical ^{1}H-NMR spectra of POSS—Cl and POSS—N_3 are shown in Figure 1. POSS—N_3 can be recognized by the peaks at (δ) 3.24 (t, 2H, POSS—$CH_2CH_2\underline{CH_2}N_3$), 1.91–1.66 (br, 9H, POSS—$CH_2\underline{CH_2}CH_2N_3$ and —$SiCH_2\underline{CH}(CH_3)_2$), 0.94 (d, 42H, —$SiCH_2CH(\underline{CH_3})_2$), and 0.70–0.59 (br, 16H, POSS—$\underline{CH_2}CH_2CH_2N_3$ and —$SiCH_2\underline{CH_2}CH(CH_3)_2$.

FTIR was also used to characterize the terminal azido group. In the FTIR spectrum of pure POSS—Cl [Figure 2(A)], there are two distinct bands at 1109 and 561 cm^{-1} corresponding to the stretching vibration of Si—O—Si and Si—Cl, which are the characteristic absorption bands of silsesquioxane cages.[30] After the reaction of POSS—Cl with NaN_3, a resulting peak at 2102 cm^{-1} appears in the spectrum of POSS—N_3, which is ascribed for the stretching vibration of the terminal azido group. On the basis of ^{1}H-NMR and FTIR, the nucleophilic substitution reaction was effectively conducted, and the terminal chloro groups were significantly transformed into azido groups.

The elemental mapping analysis of POSS—N_3 was carried out by using EDX (Figure 3). The characteristic peaks ascribed for silica, carbon, oxygen, and nitrogen elements appear in the EDX spectrum of POSS—N_3, which again indicates that the terminal chloro groups were completely transformed into azido groups.

Synthesis and Characterization of Poly(HEMA-*co*-MMA) and Poly(HEMA-*co*-MMA)-Alkyne

Statistical linear copolymers of MMA and HEMA were prepared by RAFT polymerization. The PHEMA having hydroxyl functionality was introduced as a minor component in the copolymer system in order to provide a hydrophilic nature to the resulting composites as well as to offer a site for incorporating alkyne moiety. The formation of poly(HEMA-*co*-MMA) is confirmed by the ^{1}H-NMR spectrum as shown in Figure 4(A). In the spectrum, the broad signal at 1.83–1.86 ppm (a′) is associated with the methylene groups in the backbone of the poly(HEMA-*co*-MMA) chain. The peaks around 0.85–1.04 ppm (b′) are mainly attributable to the protons of methyl groups of C—CH_3. The peak at 3.60 ppm (c′) is assigned to methyl protons of the methyl ester group, and the peaks at 3.72–3.84 ppm (e′, d′) are assigned to methylene protons adjacent to the oxygen moieties in the HEMA units. A broad peak at 4.11 ppm (f′) is ascribed for the hydroxyl proton of the HEMA segment. The introduction of HEMA in the copolymer matrix was found to be ~ 31 mol % as measured by the integrals of the respective protons (c′ with e′ and d′) in the ^{1}H-NMR spectrum [Figure 4(A)]. The functional alkynyl moiety was introduced into the

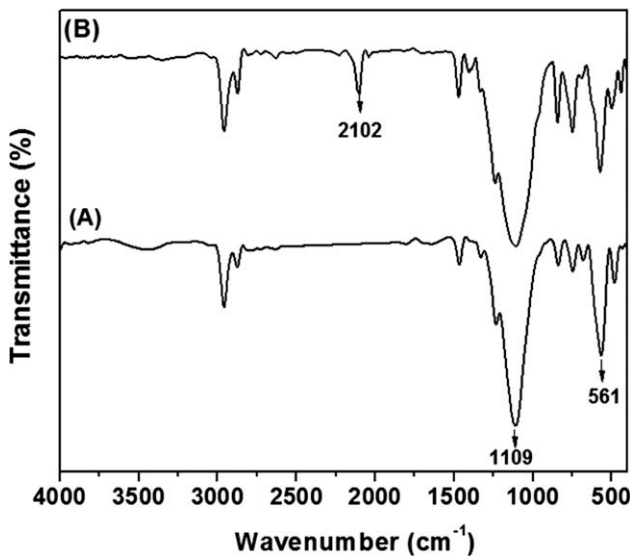

Figure 2. FTIR spectra of (A) POSS—Cl and (B) POSS—N_3.

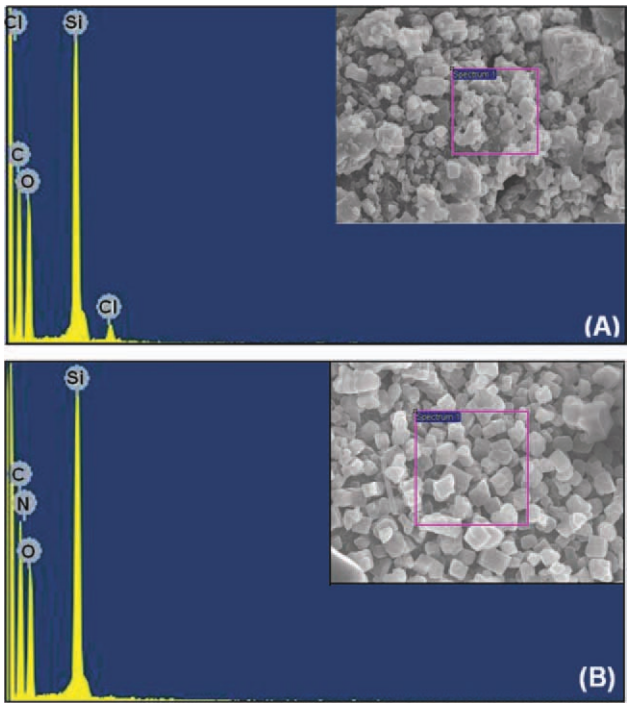

Figure 3. EDX spectrometric analysis of (A) POSS—Cl and (B) POSS—N_3. [Color figure can be viewed in the online issue, which is available at wileyonlinelibrary.com.]

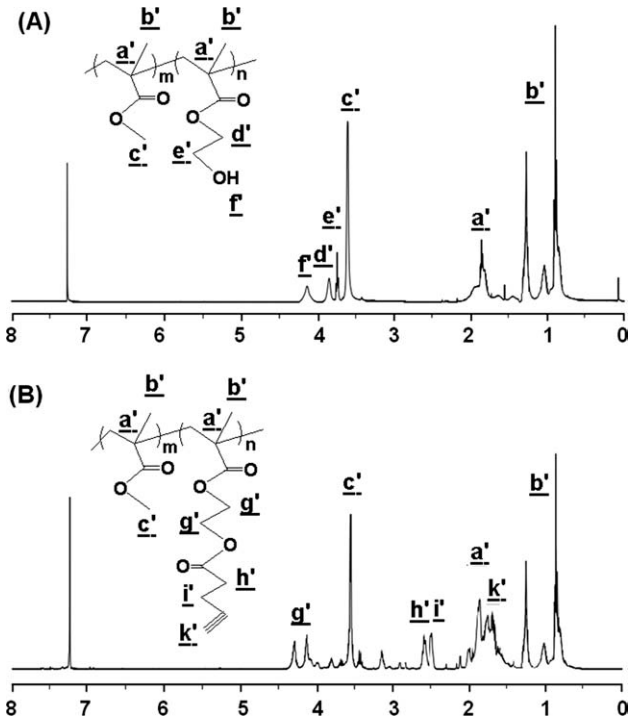

Figure 4. ^{1}H-NMR spectra of (A) poly(HEMA-*co*-MMA) and (B) poly-(HEMA-*co*-MMA)-alkyne.

polymeric backbones by esterification reaction between the hydroxyl groups on PHEMA and 4-pentynoic acid. The functional polymeric backbones, defined as poly(HEMA-*co*-MMA)-alkyne, were analyzed by ^{1}H-NMR spectroscopy. In Figure 4(B), the two broad signals at 4.17 and 4.32 ppm (g′, g′) are ascribed for the methylene protons of two ester groups (—COOC$\underline{H}_2$C$\underline{H}_2$OOC—). The peaks at 2.55 (h′) and 2.54 ppm (i′) are assigned to the resonance of the methylene protons of (—COOC$\underline{H}_2$C$\underline{H}_2$C), and peaks at the overlapping region 1.74–1.90 ppm are assigned for the polymer backbone methylene protons (a′) and acetylenic proton (k′) (—COOCH$_2$CH$_2$CC$\underline{H}$). The degree of modification of the copolymer with 4-pentynoic acid was calculated to be 27% by comparing the integrals of h′ and i′ protons of pentynoic segments with that of c′ protons of PMMA segments in the ^{1}H-NMR of poly(HEMA-*co*-MMA)-alkyne [Figure 4(B)].

The FTIR spectrum proved further the formation of poly (HEMA-*co*-MMA) as presented in Figure 5(A). A strong absorption band at 1728 cm^{-1}, which is assigned to the ester carbonyl (C=O), is associated with HEMA and MMA units.[42] The spectrum also shows two characteristic absorptions at 2952 and 1150 cm^{-1} those are attributed to the stretching vibrations of C—H and C—O—C, respectively. In addition, the characteristic broad and strong absorption band in the range of 3300–3500 cm^{-1} can be assigned to the hydroxyl groups on the HEMA units. Figure 5(B) represents the FTIR spectrum of poly-(HEMA-*co*-MMA)-alkyne, which confirms the incorporation of alkynyl groups in the poly(HEMA-*co*-MMA) chains by the esterification reaction. Similar to the parent polymer, poly-(HEMA-*co*-MMA)-alkyne shows a strong absorption band at 1730 cm^{-1}, which is ascribed to the ester carbonyl (C=O) of HEMA and MMA segments. Compared to the FTIR spectrum of poly(HEMA-*co*-MMA), the strong absorption band at 3300–3500 cm^{-1} for free hydroxyl groups completely disappeared,[42] and a new band corresponding to the stretching vibration of the alkyne groups appeared at 3301 cm^{-1} in the spectrum of poly(HEMA-*co*-MMA)-alkyne [Figure 5(B)]. These results indicate that the transformation of the hydroxyl groups to alkynyl groups on the polymer chain was successfully carried out.

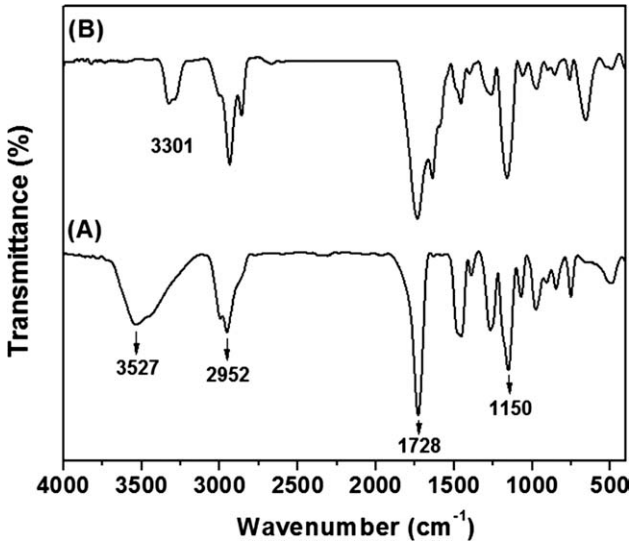

Figure 5. FTIR spectra of (A) poly(HEMA-*co*-MMA) and (B) poly-(HEMA-*co*-MMA)-alkyne.

Applied Polymer SCIENCE

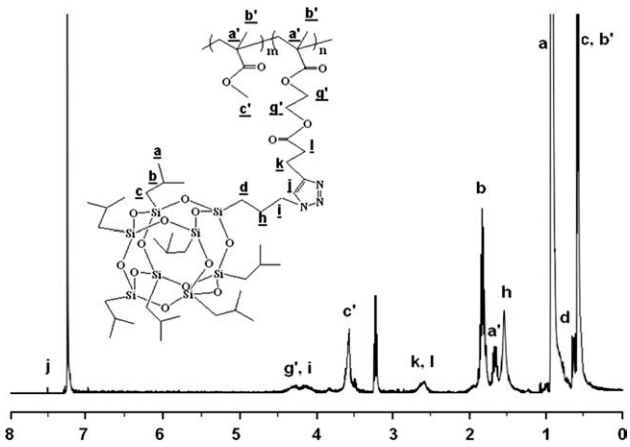

Figure 6. ^{1}H-NMR spectra of poly(HEMA-*co*-MMA)-*g*-POSS.

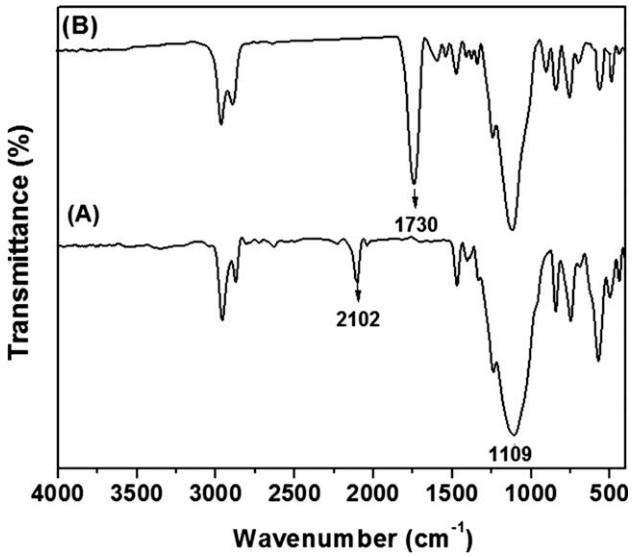

Figure 7. FTIR spectra of (A) POSS—N_3 and (B) poly(HEMA-*co*-MMA)-*g*-POSS.

Synthesis and Characterization of Poly(HEMA-*co*-MMA)-*g*-POSS

The nanocomposites of poly(HEMA-*co*-MMA)-*g*-POSS were synthesized by click reaction between the alkyne-containing poly(HEMA-*co*-MMA)-alkyne and azido-terminated POSS. Other than overlapping region from 0.58 to 1.87 ppm, characteristic proton signals for the identification of coupling product poly(HEMA-*co*-MMA)-*g*-POSS can clearly be recognized from the ^{1}H-NMR spectrum as shown in Figure 6. The signal at 7.55 ppm (j) is assigned to the proton in the triazole ring. The peaks at 4.16 and 2.61 ppm are ascribed to the methylene protons i and k adjacent to the triazole ring, respectively. The signal (c′) at 3.60 ppm is assigned to the methyl protons (—$COOCH_3$) of the MMA segment. The characteristic peaks for the POSS pendent in the matrix having shielded methylene protons adjacent to the silicon atom appear at 0.62 (d) and 0.59 (c) ppm.[36] All other representative peaks for the poly(HEMA-*co*-MMA)-*g*-POSS nanocomposites are categorically labeled in the spectrum as shown in Figure 6. The ^{1}H-NMR analysis suggests that the synthesis of poly(HEMA-*co*-MMA)-*g*-POSS was successful. Moreover, the ^{29}Si-NMR analysis of poly(HEMA-*co*-MMA)-*g*-POSS nanocomposites showed peaks at −67.58, −67.87, −96.54, −100.77, and −105.76 ppm, suggesting the presence of —O—Si—O framework in the nanocomposites.[43] The loading of POSS in the matrix was determined to be ∼ 27% from the integration of the ^{1}H-NMR spectrum.

The FTIR spectrum (Figure 7) of poly(HEMA-*co*-MMA)-*g*-POSS depicts an absorption band at 1730 cm^{-1}, which is ascribed to the stretching vibration of C=O in the PHEMA and PMMA chain. The characteristic band at 2102 cm^{-1} responsible for the azide stretching vibration has completely disappeared. The band at 1109 cm^{-1} is arisen, which is designated for Si—O—Si stretching vibration originated from the incorporation of POSS moieties. The FTIR results further prove qualitatively the presence of the POSS moieties grafted onto the poly(-HEMA-*co*-MMA) chains.

The elemental mapping analysis of poly(HEMA-*co*-MMA) and poly(HEMA-*co*-MMA)-*g*-POSS was accomplished using EDX as shown in Figure 8. The representative peaks assigned for silica, oxygen, carbon, and nitrogen elements are observed in the EDX spectrum of poly(HEMA-*co*-MMA)-*g*-POSS, which again suggests the formation of nanocomposites having the poly(HEMA-*co*-MMA) copolymer fused with POSS cage nanostructures.

XPS was used to identify the chemical composition at the surface of the modified microspheres. Figure 9 shows the XPS spectrum of the poly(HEMA-*co*-MMA)-*g*-POSS microspheres. The figure clearly shows that the synthesized nanocomposites

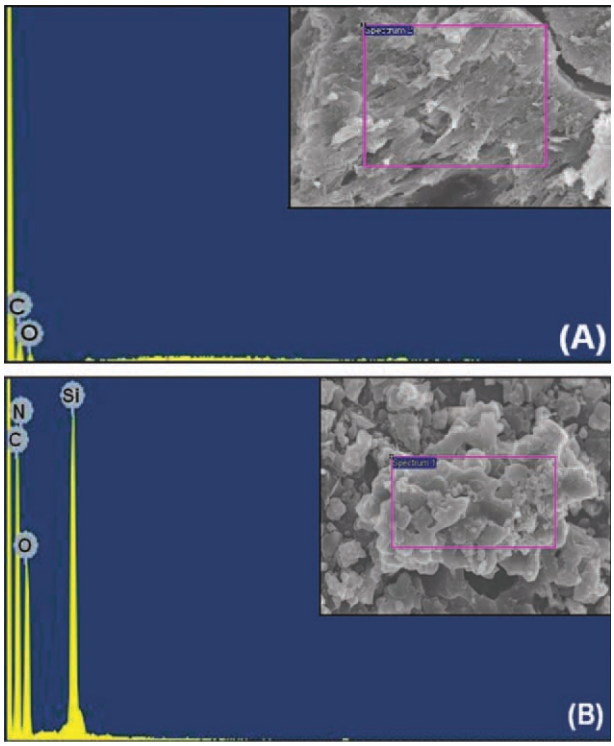

Figure 8. EDX spectrometric analysis of (A) poly(HEMA-*co*-MMA) and (B) poly(HEMA-*co*-MMA)-*g*-POSS. [Color figure can be viewed in the online issue, which is available at wileyonlinelibrary.com.]

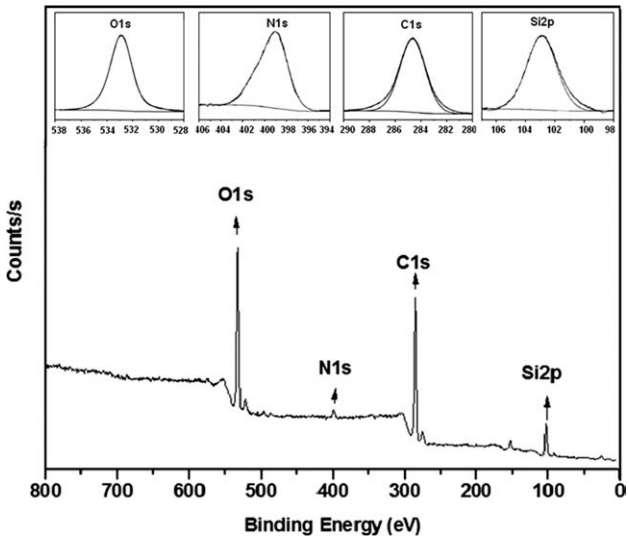

Figure 9. XPS spectra of poly(HEMA-*co*-MMA)-*g*-POSS.

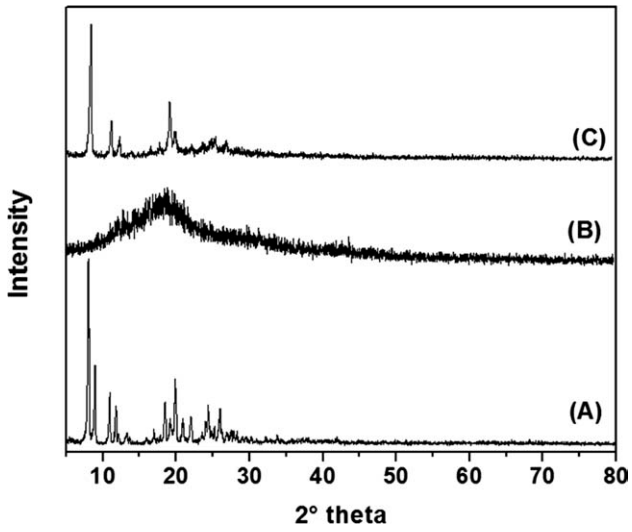

Figure 10. XRD curves of (A) POSS—Cl, (B) poly(HEMA-*co*-MMA), and (C) poly(HEMA-*co*-MMA)-*g*-POSS nanocomposites.

display characteristic signals for carbon, oxygen, nitrogen, and silicon atoms as expected for a poly(HEMA-*co*-MMA)-*g*-POSS-containing surface. The major peak component at the binding energy (BE) of about 285.10 eV is assigned to the C1s, the strongest peak at 532.7 eV corresponds to the O1s, and the peak of Si2p can be curve-fitted with BE of 103.7, which is originating from POSS. In addition, the characteristic signal for N1s can be observed at 399 eV. Thus, the XPS data clearly confirm that the attachment of poly(HEMA-*co*-MMA) onto the surface of POSS microspheres was successfully achieved.

To further investigate the structure of poly(HEMA-*co*-MMA)-*g*-POSS, the XRD measurement was carried out, and the curves are shown in Figure 10. A powder diffractogram of pure POSS—Cl is reproduced in Figure 10(A). The characteristic features of POSS show four main reflections at $2\theta = 8.2°$, 11.0°, 12.1°, and 19.0° corresponding to the lattice spacing of 10.8, 8.03, 7.31, and 4.66 Å, respectively, which are a typical XRD "fingerprint" of POSS—Cl crystals. The diffraction spectrum is very similar to those previously reported for other POSS molecules.[23,25] On the other hand, the physical structure of poly(HEMA-*co*-MMA) was observed to be amorphous [Figure 10(B)]. The XRD spectrum of poly(HEMA-*co*-MMA)-*g*-POSS as shown in the Figure 10(C) demonstrates a peak at $2\theta = 8.2°$, which is relatively less intense than its parent POSS—Cl structure. It indicates that the existence of poly(HEMA-*co*-MMA) affects the physical structure of POSS from crystalline to hybrid materials and the strong tendency of POSS toward association to form the weak crystalline organization of POSS.[32,34]

To examine the composition effect on the thermal degradation of poly(HEMA-*co*-MMA)-*g*-POSS, TGA analyses were performed for all the samples at the temperature range from 50 to 800°C. TGA curves of poly(HEMA-*co*-MMA), POSS—N_3, and poly(HEMA-*co*-MMA)-*g*-POSS samples are shown in Figure 11. The TGA of pure poly(HEMA-*co*-MMA) shows a two-step decomposition process started at relatively lower temperature (i.e., at a temperature <200°C), and 100% decomposition of the copolymer was achieved at about 450°C. However, POSS—N_3 gives a sharp continuous decomposition curve, which started at around 352°C and reached in constant weight loss of ~ 63.5% at 450°C. Because of the higher thermal stability of POSS segments, it was expected that the incorporation of POSS moieties in copolymer matrixes would improve the thermal stability of the parent copolymer. According to expectation, the TGA curve of poly(HEMA-*co*-MMA)-*g*-POSS composites shows intermediate thermal stability as shown in Figure 11(C). When the temperature was increased at around 200°C, it lost ~ 2% of its weight and further heating to about 450°C then it lost ~ 80% of its weight, which indicates that the incorporation of inorganic POSS into the copolymer matrix significantly improves the thermal property.

FE–SEM was used to investigate the morphology of poly (HEMA-*co*-MMA), POSS—N_3, and poly(HEMA-*co*-MMA)-*g*-POSS. An amorphous structure of poly(HEMA-*co*-MMA) is clearly visualized in Figure 12(A). On the other hand, the

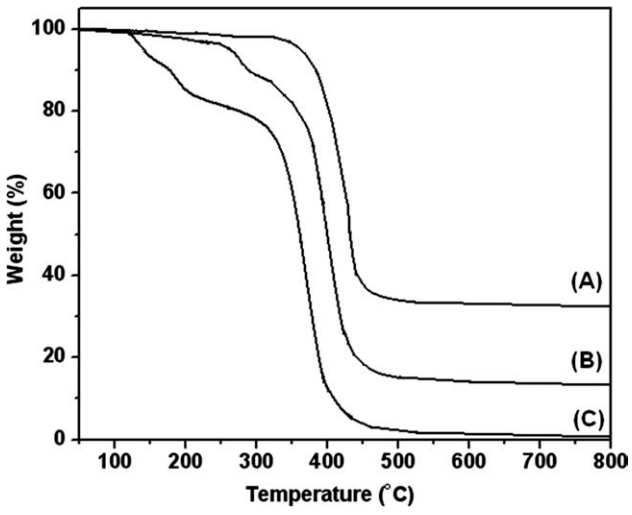

Figure 11. TGA curves of (A) poly(HEMA-*co*-MMA), (B) POSS—N_3, and (C) poly(HEMA-*co*-MMA)-*g*-POSS nanocomposites.

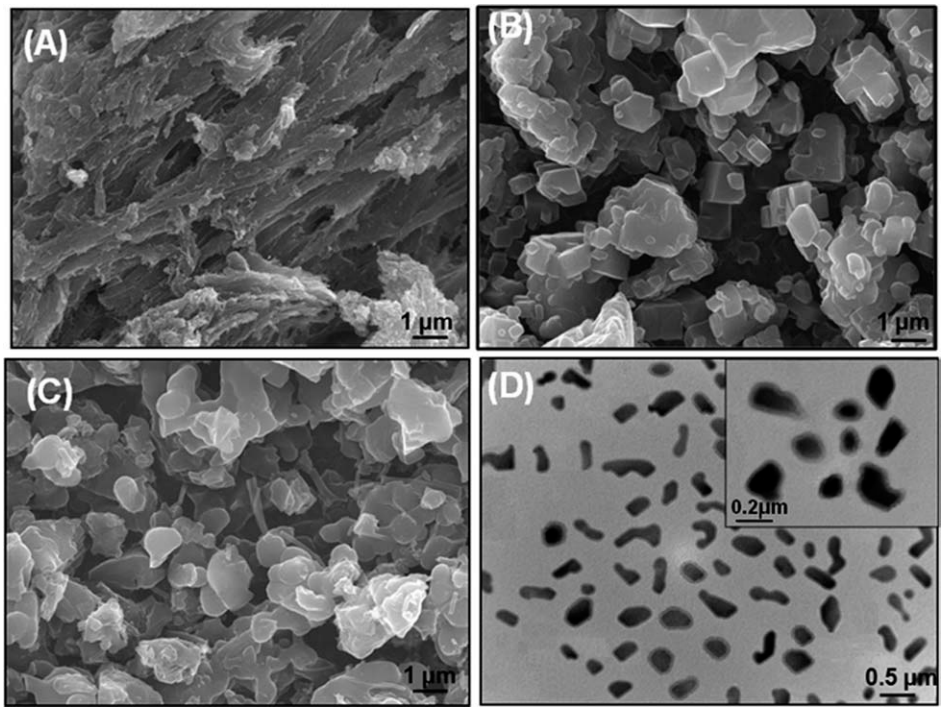

Figure 12. FE-SEM pictures of (A) poly(HEMA-*co*-MMA), (B) POSS—N_3, (C) poly(HEMA-*co*-MMA)-*g*-POSS, and (D) TEM picture of poly(HEMA-*co*-MMA)-*g*-POSS.

crystalline structure of POSS—N_3 is easily recognized from the FE–SEM image as shown in Figure 12(B). Upon the click-coupling reaction, immobilization of the poly(HEMA-*co*-MMA) copolymer onto the crystal of the POSS moiety can be distinguished by taking a close look at the FE–SEM image of the modified structure [Figure 12(C)]. The FE–SEM images suggest that the crystals of POSS—N_3 were embedded by copolymer brushes. The TEM image [Figure 12(D)] further illustrates that POSS nanocrystals were wrapped by the soft polymer layer.

The number–average molecular weight (M_n) and polydispersity index (PDI) of poly(HEMA-*co*-MMA) were found to be 16,000 g/mol and 1.61, respectively [Figure 13(A)], as determined by GPC. The GPC traces indicate that there was no apparent change in molecular weights between poly(HEMA-*co*-MMA) and poly(HEMA-*co*-MMA)-alkyne. However, from the GPC traces of poly(HEMA-*co*-MMA)-alkyne and poly(HEMA-*co*-MMA)-*g*-POSS [Figure 13(B)], it can be seen that the curve of poly(HEMA-*co*-MMA)-*g*-POSS obviously shifts to lower elution volumes, indicating that poly(HEMA-*co*-MMA)-*g*-POSS has a higher molecular weight (M_n = 17.200 g/mol, PDI = 1.64). Moreover, the GPC trace of poly(HEMA-*co*-MMA)-*g*-POSS is symmetric without a shoulder on its right side, indicating the absence of any side reactions. This result suggests that the click coupling was completed smoothly.

CONCLUSIONS

A novel hybrid poly(HEMA-*co*-MMA)-*g*-POSS was synthesized by taking advantage of RAFT polymerization and click chemistry. At first, the random copolymer of poly (HEMA-*co*-MMA) was synthesized by using MMA and HEMA in the ratio of 70 : 30 via

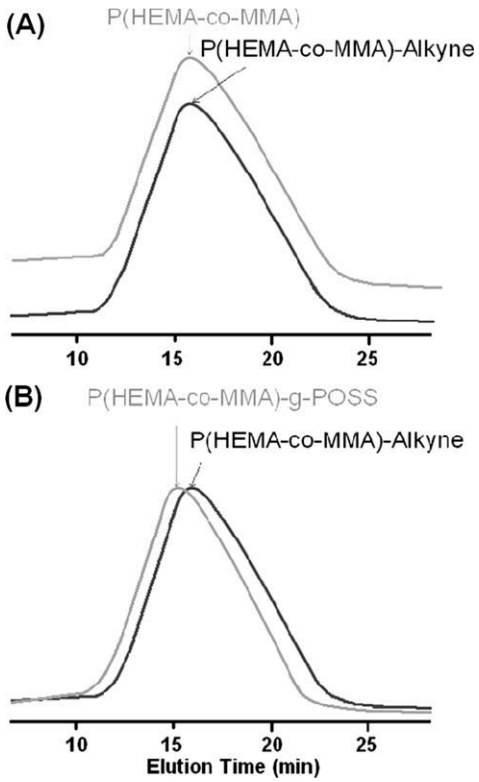

Figure 13. GPC traces of (A) poly(HEMA-*co*-MMA) and poly(HEMA-*co*-MMA)-Alkyne, (B) poly(HEMA-*co*-MMA)-alkyne and poly(HEMA-*co*-MMA)-*g*-POSS.

the RAFT polymerization technique. Alkynyl side groups were incorporated onto the polymeric backbones by esterification reaction between 4-pentynoic acid and the hydroxyl groups present on poly(HEMA-*co*-MMA). The reaction of chloropropyl-heptaisobutyl-substituted POSS with NaN_3 afforded the azide-substituted POSS (POSS—N_3). The reaction of poly(HEMA-*co*-MMA)-alkyne with POSS—N_3 using the CuBr/PMDEATA catalyst resulted in poly(HEMA-*co*-MMA)-*g*-POSS through the 1,3-dipolar cycloaddition reaction (azide-alkyne, click chemistry). The structure and properties of the nanocomposites were studied by FTIR, ^{1}H-NMR, ^{29}Si-NMR, XPS, EDX, XRD, and GPC. The XPS and EDX studies reveal the presence of silicon, oxygen, carbon, and nitrogen atoms present in the poly(HEMA-*co*-MMA)-*g*-POSS nanocomposites. The XRD spectrum of the nanocomposites indicates that the grafting of amorphous poly(HEMA-*co*-MMA) copolymers onto crystalline POSS provides hybrid-structured nanomaterials. A thick layer of polymer brushes was embedded onto the POSS cubic nanostructures, which are observed from FE–SEM and TEM images. The TGA analysis showed that the thermal property of the poly(HEMA-*co*-MMA) copolymer was improved by the incorporation of POSS nanostructures into the copolymer matrix upon covalent immobilization.

ACKNOWLEDGMENTS

This work was financially supported by the grant from the Industrial Source Technology Development Program (Project No. 10035163) of the Ministry of Knowledge Economy (MKE) of Korea and by Inter-Metropolitan Cooperation Development funded by the Presidential Committee on Regional Development.

REFERENCES

1. Achilleos, D. S.; Vamvakaki, M. *Materials* **2010,** *3*, 1981.
2. Spitalsky, Z.; Tasis, D.; Papagelis, K.; Galiotis, C. *Prog. Polym. Sci.* **2010,** *35*, 357.
3. Guptaa, A.K.; Gupta, M. *Biomaterials* **2005,** *26*, 3995.
4. Kang, J. M.; Cho, H. J.; Lee, J.; Lee, J. I.; Lee, S. K.; Cho, N. S.; Hwang, D. H.; Shim, H. K. *Macromolecules* **2006,** *39*, 4999.
5. Drazkowski, D. B; Lee, A.; Haddad, T. S.; Cookson, D. J. *Macromolecules* **2006,** *39*, 1854.
6. Wright, M. E.; Petteys, B. J.; Guenthner, A. J.; Fallis, S.; Yandek, G. R.; Tomczak, S. J.; Minton, T. K.; Brunsvold, A. *Macromolecules* **2006,** *39*, 4710.
7. Cordes, D. B.; Lickiss, P. D.; Rataboul, F. *Chem. Rev.* **2010,** *110*, 2081.
8. Kim, S. H.; Song, K. J. *Ind. Eng. Chem.* **2011,** *17*, 170.
9. Thompson, C. H.; Keeley, D. L.; Pollock, K. M.; Dvornic, P. R.; Keinath, S. E.; Dantus, M.; Gunaratne, T. C.; LeCaptain, D. J. *Chem. Mater.* **2008,** *20*, 2829.
10. Bizet, S.; Galy, J.; Gerard, J. F. *Polymer.* **2006,** *47*, 8219.
11. Gungor, E.; Bilir, C.; Hizal, G.; Tunca, U. *J. Polym. Sci. Part. A: Polym. Chem.* **2010,** *48*, 4835.
12. Xu, H.; Yang, B.; Wang, J.; Guang, S.; Li, C. *Macromolecules* **2005,** *38*, 10455.
13. Waddon, A. J.; Coughlin, E. B. *Chem. Mater.* **2003,** *15*, 4555.
14. Lim, S. K.; Hong, E. P.; Choi, H. J.; Chin, I. J. J. *Ind. Eng. Chem.* **2010,** *16*, 189.
15. Lee, W.; Ni, S.; Deng, J.; Kim, B. S.; Satija, S. K.; Mather, P. T.; Esker, A. R. *Macromolecules* **2007,** *40*, 682.
16. Ernest, A. E.; Lamb, D. W. *J. Phys.: Conf. Ser.* **2005,** *15*, 270.
17. Rayment, E. A.; Dargaville, T. R.; Shooter, G. K.; George, G. A.; Upton, Z. *Biomaterials* **2008,** *29*, 1785.
18. Karlgard, C. C. S.; Sarkar, D. K.; Jones, L. W.; Moresoli, C.; Leung, K. T. *Appl. Sur. Sci.* **2004,** *230*, 106.
19. Susdorf, T.; Del Agua, D.; Tyagi, A.; Penzkofer, A.; Garcia, O.; Sastre, R.; Costela, A.; Garcia-Moreno, I. *Appl. Phys. B.* **2007,** *86*, 537.
20. Atai, M.; Watts, D. C.; Atai, Z. *Biomaterials* **2005,** *26*, 5015.
21. Chieng, T. H.; Gan, L. M.; Chew, C. H.; Ng, S. C. *Polymer.* **1998,** *36*, 1941.
22. Ayhan, H. *J. Bioact. Compat. Polym.* **2002,** *17*, 271.
23. Fu, B. X.; Lee, A.; Haddad, T. S. *Macromolecules* **2004,** *37*, 5211.
24. Koh, K.; Sugiyama, S.; Morinaga, T.; Ohno, K.; Tsujii, Y.; Fukuda, T.; Yamahiro, M.; Iijima, T.; Oikawa, H.; Watanabe, K.; Miyashita, T. *Macromolecules* **2005,** *38*, 1264.
25. Lee, K. M.; Knight, P. T.; Chung, T.; Mather, P. T. *Macromolecules* **2008,** *41*, 4730.
26. Kim, C. K.; Kim, B. S.; Sheikh, F. A.; Lee, U. S.; Khil, M. S.; Kim, H. Y. *Macromolecules* **2007,** *40*, 4823.
27. Wu, J.; Ge, Q.; Mather, P. T. *Macromolecules,* **2010,** *43*, 7637.
28. Gao, H.; Matyjaszewski, K. *J. Am. Chem. Soc.* **2007,** *129*, 6633.
29. Chou, C. H.; Hsu, S. L.; Dinakaran, K.; Chiu, M. Y.; Wei, K. H. *Macromolecules* **2005,** *38*, 745.
30. Dijk, M.; Rijkers, D. T. S.; Liskamp, R. M. J.; Nostrum, C. F.; Hennink, W. E. *Bioconjug. Chem.* **2009,** *20*, 2001.
31. Opsteen, J. A.; Hest, J. C. M. *Chem. Commun.* **2005, 57.**
32. Wu, D.; Song, X.; Tang, T.; Zhao, H. *J. Polym. Sci. Part. A: Polym. Chem.* **2010,** *48*, 443.
33. Durmaz, H.; Dag, A.; Gursoy, D.; Demirel, A. L.; Hizal, G.; Tunca, U. *J. Polym. Sci. Part. A: Polym. Chem.* **2010,** *48*, 1557.
34. Zhang, W.; Muller, A. H. E. *Macromolecules* **2010,** *43*, 3148.
35. Gungor, E.; Bilir, C.; Durmaz, H.; Hizal, G.; Tunca, U. *J. Polym. Sci. Part. A: Polym. Chem.* **2009,** *47*, 5947.
36. Zhang, W.; Müller, A. H. E. *Polymer.* **2010,** *51*, 2133.
37. Ge, Z.; Wang, D.; Zhou, Y.; Liu, H.; Liu, S. *Macromolecules* **2009,** *42*, 2903.
38. Sumerlin, B. S.; Tsarevsky, N. V.; Louche, G.; Lee, R. Y.; Matyjaszewski, K. *Macromolecules* **2005,** *38*, 7540.
39. Ladmiral, V.; Mantovani, G.; Clarkson, G. J.; Cauet, S.; Irwin, J. L.; Haddleton, D. M. *J. Am. Chem. Soc.* **2006,** *128*, 4823.
40. O'Reilly, R. K.; Joralemon, M. J.; Hawker, C. J.; Wooley, K. L. *Chem. Eur. J.* **2006,** *12*, 6776.
41. Gondi, S. R.; Vogt, A. P.; Sumerlin, B. S. *Macromolecules* **2007,** *40*, 474.
42. Vargüün, E.; Sankir, M.; Aran, B.; Sankir, N. D.; Usanmaz, A. J. *Macromol. Sci. Part. A: Pure. Appl. Chem.* **2010,** *47*, 235.
43. Mori, H.; Lanzendofer, M. G.; Muller, A. H. E.; Klee, J. E. *Macromolecules* **2004,** *37*, 5228.